Important Notice to Authors

No further publication processing will occur until we receive your response to this proof.

Attached is a PDF proof of your forthcoming article in *Physical Review Letters*. The article accession code is LH16575.

Your paper will be in the following section of the journal: LETTERS — Condensed Matter: Electronic Properties, etc.

Please note that as part of the production process, APS converts all articles, regardless of their original source, into standardized XML that in turn is used to create the PDF and online versions of the article as well as to populate third-party systems such as Portico, Crossref, and Web of Science. We share our authors' high expectations for the fidelity of the conversion into XML and for the accuracy and appearance of the final, formatted PDF. This process works exceptionally well for the vast majority of articles; however, please check carefully all key elements of your PDF proof, particularly any equations or tables.

Figures submitted electronically as separate files containing color appear in color in the online journal. However, all figures will appear as grayscale images in the print journal unless the color figure charges have been paid in advance, in accordance with our policy for color in print (https://journals.aps.org/authors/color-figures-print).

Specific Questions and Comments to Address for This Paper

The numbered items below correspond to numbers in the margin of the proof pages pinpointing the source of the question and/or comment. The numbers will be removed from the margins prior to publication.

1. The references have been renumbered so that they appear in text in numerical order. Please verify that text citations refer to the correct renumbered references, throughout the Letter.

2. Please review the funding information section of the proof's cover letter and respond as appropriate. We must receive confirmation that the funding agencies have been properly identified before the article can publish.

3. NOTE: External links, which appear as blue text in the reference section, are created for any reference where a Digital Object Identifier (DOI) can be found. Please confirm that the links created in this PDF proof, which can be checked by clicking on the blue text, direct the reader to the correct references online. If there is an error, correct the information in the reference or supply the correct DOI for the reference. If no correction can be made or the correct DOI cannot be supplied, the link will be removed.

Titles in References

The editors now encourage insertion of article titles in references to journal articles and e-prints. This format is optional, but if chosen, authors should provide titles for *all* eligible references. If article titles remain missing from eligible references, the production team will remove the existing titles at final proof stage.

ORCIDs

Please follow any ORCID links ( ) after the authors' names and verify that they point to the appropriate record for each author.

Funding Information

Information about an article's funding sources is now submitted to Crossref to help you comply with current or future funding agency mandates. Crossref's Open Funder Registry (https://www.crossref.org/services/funder-registry/) is the definitive registry of funding agencies. Please ensure that your acknowledgments include all sources of funding for your article following any requirements of your funding sources. Where possible, please include grant and award ids. Please

carefully check the following funder information we have already extracted from your article and ensure its accuracy and completeness:

Other Items to Check

- Please note that the original manuscript has been converted to XML prior to the creation of the PDF proof, as described above. Please carefully check all key elements of the paper, particularly the equations and tabular data.
- Title: Please check; be mindful that the title may have been changed during the peer-review process.
- Author list: Please make sure all authors are presented, in the appropriate order, and that all names are spelled correctly.
- Please make sure you have inserted a byline footnote containing the email address for the corresponding author, if desired. Please note that this is not inserted automatically by this journal.
- Affiliations: Please check to be sure the institution names are spelled correctly and attributed to the appropriate author(s).
- Receipt date: Please confirm accuracy.
- Acknowledgments: Please be sure to appropriately acknowledge all funding sources.
- References: Please check to ensure that titles are given as appropriate.
- Hyphenation: Please note hyphens may have been inserted in word pairs that function as adjectives when they occur before a noun, as in "x-ray diffraction," "4-mm-long gas cell," and "R-matrix theory." However, hyphens are deleted from word pairs when they are not used as adjectives before nouns, as in "emission by x rays," "was 4 mm in length," and "the R matrix is tested."
  Note also that Physical Review follows U.S. English guidelines in that hyphens are not used after prefixes or before suffixes: superresolution, quasiequilibrium, nanoprecipitates, resonancelike, clockwise.
- Please check that your figures are accurate and sized properly. Make sure all labeling is sufficiently legible. Figure quality in this proof is representative of the quality to be used in the online journal. To achieve manageable file size for online delivery, some compression and downsampling of figures may have occurred. Fine details may have become somewhat fuzzy, especially in color figures. The print journal uses files of higher resolution and therefore details may be sharper in print. Figures to be published in color online will appear in color on these proofs if viewed on a color monitor or printed on a color printer.
- Overall, please proofread the entire *formatted* article very carefully. The redlined PDF should be used as a guide to see changes that were made during copyediting. However, note that some changes to math and/or layout may not be indicated.

Ways to Respond

- *Web:* If you accessed this proof online, follow the instructions on the web page to submit corrections.
- *Email:* Send corrections to aps-robot@luminad.com. Include the accession code LH16575 in the subject line.
- *Fax:* Return this proof with corrections to +1.855.808.3897.

If You Need to Call Us

You may leave a voicemail message at +1.855.808.3897. Please reference the accession code and the first author of your article in your voicemail message. We will respond to you via email.

Realization of a Metallic State in $1T$-TaS$_2$ with Persisting Long-Range Order of a Charge Density Wave

Xin-Yang Zhu,[1] Shi Wang,[1] Zhen-Yu Jia,[1] Li Zhu,[1] Qi-Yuan Li,[1] Wei-Min Zhao,[1] Cheng-Long Xue,[1] Yong-Jie Xu,[1]
Zhen Ma,[1] Jinsheng Wen,[1,2] Shun-Li Yu,[1,2,*] Jian-Xin Li,[1,2,†] and Shao-Chun Li[1,2,‡]

[1]*National Laboratory of Solid State Microstructures and School of Physics, Nanjing University, Nanjing 210093, China*
[2]*Collaborative Innovation Center of Advanced Microstructures, Nanjing University, Nanjing 210093, China*

Metallization of $1T$-TaS$_2$ is generally initiated at the domain boundary of a charge density wave (CDW), at the expense of its long-range order. However, we demonstrate in this study that the metallization of $1T$-TaS$_2$ can be also realized without breaking the long-range CDW order upon surface alkali doping. By using scanning tunneling microscopy, we find the long-range CDW order is always persisting, and the metallization is instead associated with additional in-gap excitations. Interestingly, the in-gap excitation is near the top of the lower Hubbard band, in contrast to a conventional electron-doped Mott insulator where it is beneath the upper Hubbard band. In combination with the numerical calculations, we suggest that the appearance of the in-gap excitations near the lower Hubbard band is mainly due to the effectively reduced on-site Coulomb energy by the adsorbed alkali ions.

$1T$-TaS$_2$ has been extensively studied for decades as a unique transition metal dichalcogenide compound hosting the ground state of a Mott insulator [1–3] intertwined with a commensurate charge density wave (CDW) [4]. A series of temperature dependent CDW orders have been discovered [2,5,6], and a large electron-phonon coupling has been demonstrated in $1T$-TaS$_2$ which may be associated with the formation of the CDW state [7,8]. Realization of superconductivity in $1T$-TaS$_2$, particularly by doping [9,10] or applying pressure [11], further makes it an alternate model system to study the interplay between superconductivity and strong correlation physics [12]. Recently, $1T$-TaS$_2$ has attracted more attention because of the theoretical prediction and experimental exploration of the possible quantum spin liquid state [13–18].

In general, the band filling n, the on-site Coulomb energy U, and the one-electron bandwidth W together drive the Mott insulator transition in a coordinated manner [19]. Unlike other conventional Mott insulators, the on-site Coulomb energy U in $1T$-TaS$_2$ is not large enough to directly open a Mott gap. The essential ingredient here is that the presence of the commensurate CDW with a David star structure isolates a narrow energy band near the Fermi energy [20]. This band mainly consists of the $5d$ orbitals at the center of the David star [21]. Therefore, a moderate U can open a Mott gap in this narrow band which is half filled.

The metallization of $1T$-TaS$_2$ is believed to be accompanied with the breaking of the long-range CDW order; i.e., the metallic phase starts to initiate at the domain boundaries of the CDW state [22], where the long-range order is simultaneously destructed. The metallization has been realized experimentally via applying pressure [11], chemical substitution [23], ultrafast laser pulses [24], current excitation [25,26] or applying a pulse voltage [27], which induce domain boundaries and suppress the long-range CDW order [11,23–27]. However, the nature of Mott insulator-metal transition in $1T$-TaS$_2$ still remains elusive, partially owing to the complex correlation between the Mott insulator and the CDW state. It is not even clear whether the collapse of the Mott gap is necessarily connected with the destruction of the long-range CDW order.

In this work, we explore the Mott insulator-metal transition of $1T$-TaS$_2$ upon surface doping by alkali K atoms. The K atoms deposited onto the surface will transfer electrons to the host lattice to increase the band filling [28], and the left K$^+$ ions effectively modify the crucial parameters U/W of the Mott insulator-metal transition. In the meantime, such a method induces a negligible orbital effect, which may complicate the related physics [29]. By using scanning tunneling microscopy or spectroscopy (STM/STS), we directly characterize the electronic state evolution from Mott insulator to metal. Surprisingly, we find the long range CDW order is always persisting during the metallization, indicating that such Mott insulator-metal transition is fundamentally different from that triggered by the domain boundaries of the CDW [23,30–32]. The metallization is found to arise from the filling up of the Mott gap by additional in-gap excitations induced by the surface alkali doping. Though this phenomenon is common for conventional Mott insulators, such as the doped high-T_c cuprates [33], we observe that the in-gap

81 excitation is unexpectedly located above the lower Hubbard
82 band (LHB), which is underneath the upper Hubbard band
83 (UHB) in the case of electron doped conventional Mott
84 insulators. Considering that the Mott insulating state in
85 $1T$-TaS$_2$ is derived from the isolated narrow band due to the
86 CDW, we construct a single-band Hubbard model with a
87 site-dependent U to account for the possible effect of the
88 surface K$^+$ ions. Using the cluster perturbation theory
89 (CPT), we calculate the spectral function of electrons and
90 find qualitative consistency with experiments. We therefore
91 suggest that the K$^+$ ions adsorbed at the center of the David
92 star would effectively reduce the Coulomb energy U and
93 result in the appearance of the in-gap excitations near
94 the LHB.

95 The $1T$-TaS$_2$ single crystal was grown by the chemical
96 vapor transport method. STM and STS measurements were
97 carried out in a low-temperature scanning tunneling micro-
98 scope (Unisoku Co.) at ∼4.2 K in ultrahigh vacuum
99 (UHV), with the base pressure of 1×10^{-10} mbar. The
100 clean surface of $1T$-TaS$_2$ was achieved by cleaving the
101 sample *in situ* in UHV. The sample was kept at ∼4.2 K and
102 then quickly transferred to the evaporation chamber prior to
103 K deposition. The K source (SAES, Alkali metal dispenser)
104 was heated to ∼650 °C, and the atomic flux of K is
105 estimated to be ∼0.005 ML/s. After the deposition, the
106 sample was transferred to the STM stage for a scan without
107 annealing. Because of the strong enough bonding to the
108 $1T$-TaS$_2$ surface, the K atoms are static during a normal
109 scan. STM topographic images were collected under the
110 constant current mode. STS dI/dV spectra were taken with
111 a lock-in amplifier and a typical ac modulation of 10 mV
112 and 879 Hz.

113 The bulk $1T$-TaS$_2$ crystal has a layered structure [34].
114 The Ta atomic layer is sandwiched between two S atomic
115 layers. In the normal state, the Ta atoms sit at the center of
116 the approximate S octahedra. In the CDW phase, $1T$-TaS$_2$
117 forms a $\sqrt{13} \times \sqrt{13}$ superstructure composed of the David
118 star clusters, as shown in Fig. 1(a). A high-resolution STM
119 image taken in this CDW phase is displayed in Fig. 1(b).
120 Close examination reveals the position of the topmost
121 S atoms in each David star cluster. There exist three
122 inequivalent types of Ta atoms in the unit cell designated
123 by different colors in Figs. 1(b) and 1(c).

124 The dI/dV spectrum, which is proportional to the
125 electron local density of states (LDOS), is taken on the
126 $1T$-TaS$_2$ surface and plotted in Fig. 1(d). The UHB and
127 LHB can be clearly identified as the peaks marked in the
128 dI/dV curve, in agreement with the previous reports [35].
129 These spectroscopic features can be captured by DFT
130 calculations including the on-site Hubbard U correction
131 in a Hartree-Fock approximation [36]. The peak below the
132 LHB is referred to as the valence band (VB). The CDW gap
133 thus locates between the LHB and the VB [37–39]. The
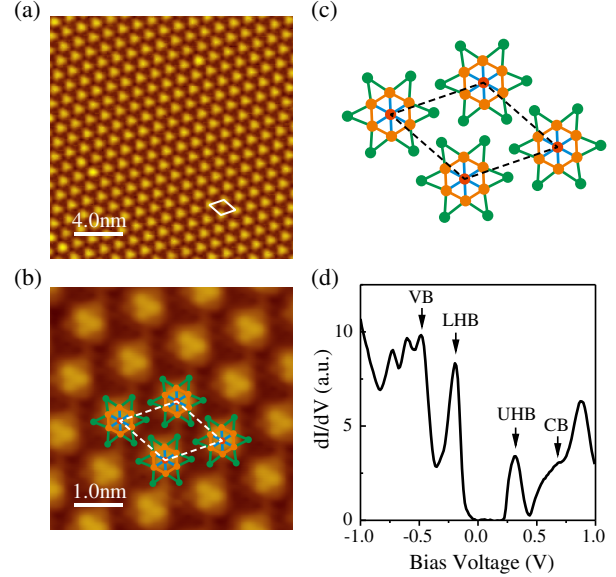134 conduction band (CB) is located above the UHB.

FIG. 1. (a) STM topographic image (40×40 nm^2) taken at ∼4.2 K on the pristine $1T$-TaS$_2$ surface, showing the $\sqrt{13} \times \sqrt{13}$ periodicity. $U = +1.0$ V and $I_t = 100$ pA. (b) High-resolution STM image (5×5 nm^2) showing the atomic structure of the David star. The David star model is overlaid on the STM image. $U = +100$ mV and $I_t = 200$ pA. Individual S atoms are re-solved as small blobs in each David star cluster, which enables us to identify the position of Ta atoms underneath. (c) Schematic of the top view David star structure. Different colors represent the inequivalent Ta atoms derived from different positions in the David star cluster. (d) Spatially averaged dI/dV spectrum acquired with $U = +500$ mV and $I_t = 100$ pA.

135 The evolution of dI/dV spectra upon K doping to the
136 $1T$-TaS$_2$ surface is plotted in Fig. 2(a). Initially, the Fermi
137 level starts to lift slightly towards the UHB. Yet, the whole
138 characteristics of the spectra do not seem to change, as
139 exemplified by the plot of 0.05 ML in Fig. 2(a). This can be
140 interpreted as that the K electrons are trapped by the surface
141 impurities for a small amount of K deposition. When more
142 K atoms are deposited, e.g., from 0.08 ML on in Fig. 2(a),
143 additional excitations become identifiable within the Mott
144 gap, indicating that the K electrons dope the Mott insulator
145 effectively. An important feature is that these additional
146 excitations are close to the LHB. They keep growing until
147 the whole Mott gap is filled up when the coverage reaches
148 ∼0.32 ML. At this coverage, the collected dI/dV results
149 exhibit the uniform metallic state on the whole $1T$-TaS$_2$
150 surface, and thus the surface undergoes a transition from
151 Mott insulator to metal. To quantitatively analyze the
152 electronic evolution, we define the CDW gap Δ_{CDW} as
153 the width from the VB peak to the LHB peak, Δ_{Mott} from
154 the LHB peak to the UHB peak, and Δ_0 for the zero
155 intensity region accordingly, as illustrated in Fig. 2(b).
156 Figure 2(c) shows the magnitude of the three gaps as a
157 function of the K coverage. At first, Δ_0 is closed at
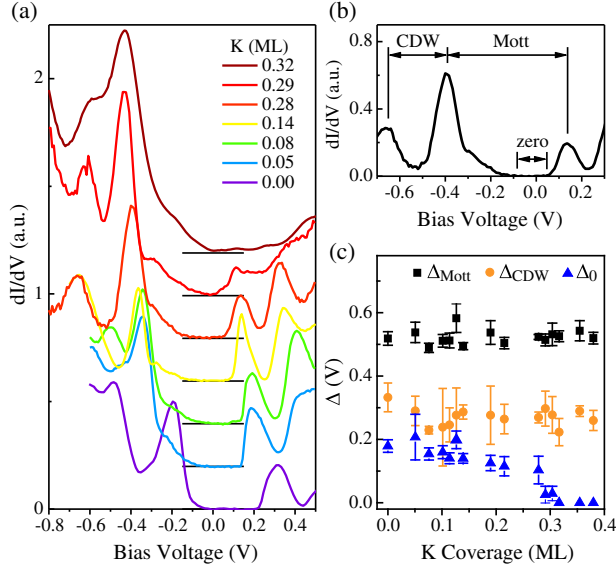158 ∼0.32 ML. Second, during the Mott insulator-metal

F2:1 FIG. 2. (a) dI/dV spectra taken on the $1T$-TaS$_2$ surface with
F2:2 different K coverage. The data were acquired with $U =$
F2:3 $+500$ mV and $I_t = 100$ pA. (b) Definition of the three gaps
F2:4 in the $1T$-TaS$_2$ dI/dV spectrum. Δ_{Mott} is defined as the width
F2:5 between the two Hubbard peaks, Δ_{CDW} the width between LHB
F2:6 and VB peaks, and Δ_0 the width of the zero-intensity region
F2:7 within the Mott gap. (c) Dependence of the magnitude of the
F2:8 three gaps on the K coverage.

159 transition, the UHB and LHB peaks are both identifiable,
160 and the magnitude of Δ_{Mott} does not prominently change.
161 Third, no change is observed in the magnitude of Δ_{CDW}.
162 The peak of VB remains at a fixed position relative to the
163 LHB as the K coverage increases. Therefore, the electron
164 doping by K atoms on the surface of $1T$-TaS$_2$ does not
165 close the CDW gap in the process of the metallization.
166 **1** We further explore the effects of the alkali doping on the
167 long-range CDW order. Figure 3(a) shows the STM topo-
168 graphic image of the $1T$-TaS$_2$ surface with a low coverage
169 of K atoms. The identified David star clusters form a
170 triangular structure as traced by the yellow dashed mesh
171 where each cluster is denoted by the crossing. The K atom
172 is adsorbed preferentially on top of the center of the David
173 star cluster. Then, we present the image of the surface
174 covered with a high coverage of ~ 0.4 ML in Fig. 3(b),
175 where all the K atoms are still in a single-atom format
176 without clustering. Figure 3(c) shows the zoom-in image of
177 the white square region in Fig. 3(b), where the black mesh
178 and dots represent the David star structure and adsorbed K
179 atoms, respectively. We find that 152 of the total 162 K
180 atoms are located at the David star center. This analysis
181 suggests that the long-range CDW order still remains at this
182 coverage. Moreover, Fig. 3(d), the Fourier transform of
183 Fig. 3(b), shows that the peak corresponding to the CDW
184 periodicity as marked by the blue circle is rather sharp,
185 indicating the long-range CDW order without domain
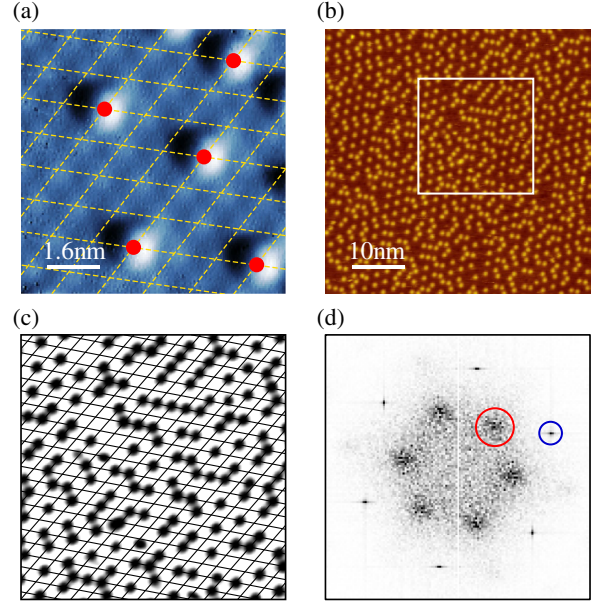186 boundary. It is a remarkable result because the whole

FIG. 3. (a) Small-scale STM current image (8×8 nm^2) taken F3:1
at the $1T$-TaS$_2$ surface with a low K coverage. The David star F3:2
structure is highlighted by the yellow dashed mesh, and the F3:3
adsorption sites of K at the David star center are marked by red F3:4
dots. (b) Large-scale STM topographic image (50×50 nm^2) F3:5
taken on the $1T$-TaS$_2$ surface with the K coverage of ~ 0.4 ML. F3:6
$U = +1.0$ V and $I_t = 100$ pA. (c) The adsorption sites of K F3:7
atoms extracted from the white square region in (b). The black F3:8
dots represent the positions of K atoms, and the parallel lines the F3:9
lattice of the $1T$-TaS$_2$ substrate. (d) Fourier transform of the STM F3:10
image (b). The blue and red circles mark the peaks originated F3:11
from the surface K atoms. F3:12

$1T$-TaS$_2$ surface is already metallic at this coverage. In 187
previous studies of the Mott insulator-metal transition in 188
$1T$-TaS$_2$, such as that induced by applying pressure [11], 189
chemical substitution [23], ultrafast laser pulses [24], 190
current excitation [25,26] or applying a pulse voltage 191
[27], the domain boundaries were found to be responsible 192
to the formation of the metallic state. However, in the K 193
doped $1T$-TaS$_2$ surface, the formation of the domain 194
boundary is not necessary for the metallization, and this 195
Mott insulator-metal transition occurs without the destruc- 196
tion of the long-range CDW order. 197

With the presence of the long-range CDW order in mind, 198
we expect that a single-band Hubbard model would capture 199
the main physics of the Mott insulator-metal transition, as 200
the isolated narrow band still exists. Figure 4(a) schemati- 201
cally illustrates the spectral weight transfer in the conven- 202
tional Hubbard model with electron doping [40,41]. In the 203
large U ($U/t \to \infty$) limit and with half filling, the spectral 204
weight integrals of the LHB and UHB divided by the 205
number of lattice sites are both equal to 1. When extra 206
electrons are introduced into this system, both the possi- 207
bilities of creating holes (removing electrons from the 208
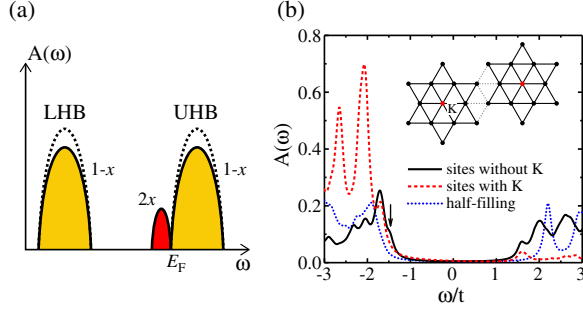LHB) and double occupancies (adding electrons into the 209

(a)

(b)

F4:1 FIG. 4. (a) Schematic of the spectral weight transfer in the local
F4:2 limit for an electron-doped Hubbard model with a uniform U.
F4:3 (b) Spectra calculated by the cluster perturbation theory. The
F4:4 spectrum of the half-filled system is illustrated by the dotted
F4:5 (blue) line, while the spectra in the sites with and without K^+ ions
F4:6 which are simulated by different U (see the text) after one-
F4:7 electron doping in the 13-site cluster are illustrated by the dashed
F4:8 (red) line and solid (black) line, respectively. The arrrow indicates
F4:9 the in-gap excitation near the LHB. The inset shows the shape of
F4:10 clusters used in the theoretical calculations.

210 UHB) are reduced by the doping concentration x. Thus, the
211 total spectral weight of LHB and UHB are changed to
212 $1 - x$, and the reduced spectral weight shifts to the bottom
213 of the UHB, which is just below the Fermi level, as
214 illustrated in Fig. 4(a). However, this picture clearly
215 contradicts the experimental results as shown in Fig. 2,
216 because the additional excitation is observed near the top of
217 LHB and the spectral intensity of LHB is increased.
218   As mentioned above, the experimental results show that
219 each K^+ ion is located at the center of one David star, so the
220 electron concentration for the David stars with K^+ ions is
221 larger than those without K^+ ions due to the Coulomb
222 attraction of the positive charge of K^+, which is equivalent
223 to the decrease of the effective repulsive interactions
224 between electrons in the lattice sites with K^+ ions.
225 Thus, we construct a site-dependent Hubbard model as
226 described by

$$H = \sum_{\langle i,j \rangle \sigma} t_{ij}(c_{i\sigma}^{\dagger}c_{j\sigma} + \text{H.c.}) + \sum_{i} U_i n_{i\uparrow}n_{i\downarrow}, \quad (1)$$

228 where t_{ij} is the effective hopping between the nearest-
229 neighbor David stars and U_i the effective on-site Coulomb
230 repulsion. In theoretical calculations, we set t_{ij} to be
231 uniform $t_{ij} = t$, and $U_i = 10t$ for David stars without
232 K^+ deposition and $U_i = 2t$ for David stars with K^+
233 deposition. We calculate the LDOS by using the cluster
234 perturbation theory [41–43]. As shown in the inset of
235 Fig. 4(b), to preserve the rotation symmetry of the
236 triangular lattice, we use 13-site clusters and set the K^+
237 ion at the center of each cluster. It is noteworthy that each
238 site in the model represents a David star in the real material.
239 The theoretical results of LDOS at half filling and with
240 one electron doping in the 13-site clusters are shown in

241 Fig. 4(b). For the half-filling system, a Mott gap of about $4t$
242 is clearly seen, while for the doped system, there exist
243 additional excitations inside the Mott gap and close to the
244 LHB for the David stars without K^+ deposition. This
245 feature is qualitatively consistent with the experimental
246 observation. We also present the LDOS for the David stars
247 with K^+ deposition in Fig. 4(b). Since the effective
248 interaction U becomes small, most spectral weights are
249 transferred to the low-energy part. The coupling between
250 the David stars with and without K^+ deposition causes the
251 redistribution of the spectral weight on the David stars
252 without K^+ deposition, which leads to the appearance of
253 the in-gap excitations near the LHB as observed in
254 experiment.
255   In summary, we realize a novel Mott insulator-metal
256 transition in the surface of the CDW-assisted Mott insulator
257 $1T\text{-TaS}_2$ by surface alkali doping. Different from those
258 triggered by the domain boundaries of the CDW state in
259 which the long-range order of the CDW is destructed, we
260 find that the long-range CDW order here is preserved all the
261 way in the metallization, and the transition results from
262 the filling up of the Mott gap by the in-gap additional
263 excitations induced by the surface alkali doping. Moreover,
264 the in-gap additional excitations are found to locate above
265 the LHB, in contrast to the case of electron doped conven-
266 tional Mott insulators where it is underneath the UHB.
267 Making use of the numerical calculations of the site-
268 dependent Hubbard model, we suggest that it is the K^+
269 ions adsorbed at the center of David stars that efficiently
270 modulate the Coulomb energy and thus result in the
271 appearance of the in-gap excitations near the LHB. This
272 study paves the way toward the understanding of the
273 correlation between a CDW and Mott insulators in tran-
274 sition metal dichalcogenides.

280   X. Y. Z. and S. W. contributed equally to this work.

281 *Note added.*—This work is premised on the assumption that
282 the insulating state in $1T\text{-TaS}_2$ is due to Mott gap opening
283 in the narrow band crossing the Fermi level, and the
284 assumption that the physics in essentially 2D. There are
285 other proposals that the metal-insulator transition is related
286 to stacking order changes because of the strong interlayer
287 coupling [49].

288 *slyu@nju.edu.cn
291 †jxli@nju.edu.cn
292 ‡scli@nju.edu.cn
293

[1] E. Tosatti and P. Fazekas, J. Phys. (Paris), Colloq. **37**, C4 (1976).

[2] P. Fazekas and E. Tosatti, Philos. Mag. B **39**, 229 (1979).

[3] P. Fazekas and E. Tosatti, Physica **99(B+C)**, 183 (1980).

[4] R. E. Thomson, U. Walter, E. Ganz, J. Clarke, A. Zettl, P. Rauch, and F. J. DiSalvo, Phys. Rev. B **38**, 10734 (1988).

[5] F. J. Di Salvo, J. A. Wilson, B. G. Bagley, and J. V. Waszczak, Phys. Rev. B **12**, 2220 (1975).

[6] C. B. Scruby, P. M. Williams, and G. S. Parry, Philos. Mag. **31**, 255 (1975).

[7] G. Benedek, F. Hofmann, P. Ruggerone, G. Onida, and L. Miglio, Surf. Sci. Rep. **20**, 1 (1994).

[8] G. Benedek, G. Brusdeylins, F. Hofmann, P. Ruggerone, J. Toennies, R. Vollmer, and J. Skofronick, Surf. Sci. **304**, 185 (1994).

[9] Y. Liu, R. Ang, W. J. Lu, W. H. Song, L. J. Li, and Y. P. Sun, Appl. Phys. Lett. **102**, 192602 (2013).

[10] L. J. Li, W. J. Lu, X. D. Zhu, L. S. Ling, Z. Qu, and Y. P. Sun, Europhys. Lett. **97**, 67005 (2012).

[11] B. Sipos, A. F. Kusmartseva, A. Akrap, H. Berger, L. Forró, and E. Tutiš, Nat. Mater. **7**, 960 (2008).

[12] D. F. Shao, R. C. Xiao, W. J. Lu, H. Y. Lv, J. Y. Li, X. B. Zhu, and Y. P. Sun, Phys. Rev. B **94**, 125126 (2016).

[13] P. W. Anderson, Mater. Res. Bull. **8**, 153 (1973).

[14] M. Klanjšek, A. Zorko, R. Žitko, J. Mravlje, Z. Jagličić, P. K. Biswas, P. Prelovšek, D. Mihailovic, and D. Arčon, Nat. Phys. **13**, 1130 (2017).

[15] K. T. Law and P. A. Lee, Proc. Natl. Acad. Sci. U.S.A. **114**, 6996 (2017).

[16] M. Kratochvilova, A. D. Hillier, A. R. Wildes, L. Wang, S.-W. Cheong, and J.-G. Park, npj Quantum Mater. **2**, 42 (2017).

[17] A. Ribak, I. Silber, C. Baines, K. Chashka, Z. Salman, Y. Dagan, and A. Kanigel, Phys. Rev. B **96**, 195131 (2017).

[18] Y. J. Yu, Y. Xu, L. P. He, M. Kratochvilova, Y. Y. Huang, J. M. Ni, L. Wang, S.-W. Cheong, J.-G. Park, and S. Y. Li, Phys. Rev. B **96**, 081111(R) (2017).

[19] M. Imada, A. Fujimori, and Y. Tokura, Rev. Mod. Phys. **70**, 1039 (1998).

[20] R. Brouwer and F. Jellinek, Physica (Amsterdam) **99(B+C)**, 51 (1980).

[21] K. Rossnagel and N. V. Smith, Phys. Rev. B **73**, 073106 (2006).

[22] J. Skolimowski, Y. Gerasimenko, and R. Žitko, Phys. Rev. Lett. **122**, 036802 (2019).

[23] S. Qiao, X. Li, N. Wang, W. Ruan, C. Ye, P. Cai, Z. Hao, H. Yao, X. Chen, J. Wu, Y. Wang, and Z. Liu, Phys. Rev. X **7**, 041054 (2017).

[24] L. Stojchevska, I. Vaskivskyi, T. Mertelj, P. Kusar, D. Svetin, S. Brazovskii, and D. Mihailovic, Science **344**, 177 (2014).

[25] I. Vaskivskyi, I. A. Mihailovic, S. Brazovskii, J. Gospodaric, T. Mertelj, D. Svetin, P. Sutar, and D. Mihailovic, Nat. Commun. **7**, 11442 (2016).

[26] M. Yoshida, R. Suzuki, Y. Zhang, M. Nakano, and Y. Iwasa, Sci. Adv. **1**, e1500606 (2015).

[27] L. Ma, C. Ye, Y. Yu, X. F. Lu, X. Niu, S. Kim, D. Feng, D. Tománek, Y.-W. Son, X. H. Chen, and Y. Zhang, Nat. Commun. **7**, 10956 (2016).

[28] C. Ramírez and W. Schattke, Surf. Sci. **482**, 424 (2001).

[29] C. Pettenkofer and W. Jaegermann, Phys. Rev. B **50**, 8816 (1994).

[30] K. Rossnagel, E. Rotenberg, H. Koh, N. V. Smith, and L. Kipp, Phys. Rev. Lett. **95**, 126403 (2005).

[31] R. Ang, Y. Tanaka, E. Ieki, K. Nakayama, T. Sato, L. J. Li, W. J. Lu, Y. P. Sun, and T. Takahashi, Phys. Rev. Lett. **109**, 176403 (2012).

[32] E. Lahoud, O. N. Meetei, K. B. Chaska, A. Kanigel, and N. Trivedi, Phys. Rev. Lett. **112**, 206402 (2014).

[33] P. Cai, W. Ruan, Y. Peng, C. Ye, X. Li, Z. Hao, D.-H. L. X. Zhou, and Y. Wang, Nat. Phys. **12**, 1047 (2016).

[34] J. A. Wilson and A. D. Yoffe, Adv. Phys. **18**, 193 (1969).

[35] D. Cho, Y.-H. Cho, S.-W. Cheong, K.-S. Kim, and H. W. Yeom, Phys. Rev. B **92**, 085132 (2015).

[36] P. Darancet, A. J. Millis, and C. A. Marianetti, Phys. Rev. B **90**, 045134 (2014).

[37] N. V. Smith, S. D. Kevan, and F. J. DiSalvo, J. Phys. C **18**, 3175 (1985).

[38] F. Zwick, H. Berger, I. Vobornik, G. Margaritondo, L. Forró, C. Beeli, M. Onellion, G. Panaccione, A. Taleb-Ibrahimi, and M. Grioni, Phys. Rev. Lett. **81**, 1058 (1998).

[39] P. A. Lee, N. Nagaosa, and X.-G. Wen, Rev. Mod. Phys. **78**, 17 (2006).

[40] H. Eskes, M. B. J. Meinders, and G. A. Sawatzky, Phys. Rev. Lett. **67**, 1035 (1991).

[41] W.-H. Leong, S.-L. Yu, T. Xiang, and J.-X. Li, Phys. Rev. B **90**, 245102 (2014).

[42] D. Sénéchal, D. Perez, and M. Pioro-Ladrière, Phys. Rev. Lett. **84**, 522 (2000).

[43] See Supplemental Material at http://link.aps.org/supplemental/10.1103/PhysRevLett.000.000000 for details about the theoretical calculations, which includes Refs. [44–48].

[44] M. G. Zacher, R. Eder, E. Arrigoni, and W. Hanke, Phys. Rev. Lett. **85**, 2585 (2000).

[45] D. Sénéchal and A.-M. S. Tremblay, Phys. Rev. Lett. **92**, 126401 (2004).

[46] S.-L. Yu, X. C. Xie, and J.-X. Li, Phys. Rev. Lett. **107**, 010401 (2011).

[47] J. Kang, S.-L. Yu, T. Xiang, and J.-X. Li, Phys. Rev. B **84**, 064520 (2011).

[48] S.-L. Yu, W. Wang, Z.-Y. Dong, Z.-J. Yao, and J.-X. Li, Phys. Rev. B **98**, 134410 (2018).

[49] S.-H. Lee, J. S. Goh, and D. Cho, Phys. Rev. Lett. **122**, 106404 (2019).